DOI: 10.1002/ejic.200601175

Structural and Theoretical Insights into Metal–Scorpionate Ligand Complexes

Matthias Schwalbe,[a] Prokopis C. Andrikopoulos,[a] David R. Armstrong,[a] John Reglinski,*[a] and Mark D. Spicer*[a]

Keywords: Nitric oxide / Soft scorpionates / Molybdenum / Tungsten / Molecular orbital calculations

The syntheses of the complexes $[M(Tm^{Me})(CO)_2(NO)]$ (M = Mo, W) by reaction of $NOBF_4$ with $[M(Tm^{Me})(CO)_3]^-$ are reported and their spectroscopic characterisation and crystal structures are described. The analogous Cr complex could not be prepared by this methodology. The complexes adopt the expected pseudo-octahedral geometry. Complexes $[M(L)(CO)_2(NO)]$ (M = Cr, Mo, W; L = Cp, Tp and Tm^{Me}) together with the hypothetical $[Mo(CO)_2(NO)]^+$ cation were subjected to DFT calculations. Geometry-optimised structures closely parallel the crystallographic determinations and indicate that the complex $[Cr(Tm^{Me})(CO)_2(NO)]$ is not inherently unstable. The DFT calculations allow the assignment of the C–O and N–O stretches in the IR spectrum and give insight into both the M–NO bonding and the metal to tripodal ligand bonding. The electron-donor strengths are confirmed to lie in the order $Tm^{Me} > Tp > Cp$. A side reaction of the B–H moiety of the Tm^{Me} anion with NO^+ results in the isolation of the dimethylformamide adduct of (trismethimazolyl)borane, providing further evidence that the reaction pathways of the Tm^R ligands are more varied and less passive than in the chemistry of the nitrogen-based scorpionates.

Introduction

While a ligand may grow in popularity on the basis of a straightforward, high-yield preparation, and the ready synthesis of a suite of interesting complexes, its full utility can only be realised when a deeper understanding of the metal–ligand interaction is attained. Such an understanding leads in turn to an ability to predict the influence on a given metal centre, the chemistry it will support and the chemical frontiers which can be challenged by its use. Ground-breaking discoveries in chemistry, such as the first dihydrogen species, $[W(CO)_3(P\mathit{i}Pr_3)_2(H_2)]$,[1] and the unexpectedly stable alkyne complexes (e.g. $[CpMo(CO)(RC{\equiv}CR')_2]^+$)[2] are more easily rationalised in retrospect, when the various supporting ligand–metal interactions are understood.

The character of the ligand is usually described in terms of steric and electronic influences. Steric bulk can be readily altered, and demands only that the modified ligand does not preclude the formation of the principal metal–ligand bond. The result is to constrain the remaining coordination sites. Thus, with PEt_3, the complex $[Pt^0(PEt_3)_4]$ can be formed, while with the bulkier phosphane PCy_3, only three phosphanes are able to coordinate to the metal centre and $[Pt^0(PCy_3)_3]$ is formed.[3] Electronic properties are more complex, although ultimately the main concern is usually the donor strength. This can be influenced by inductive effects (basicity) and by the donor/acceptor properties of the ligand. Furthermore, terms such as hardness and softness and ligand-field strength can also be used in this context to explain aspects of ligand behaviour. However, what is clear is that these various steric and electronic factors rarely act in isolation, but rather a complex inter-relationship exists between them.

Many popular ligand systems are designed in such a way that the user can tailor both effects. Foremost amongst these ligand systems are the poly(azolyl)borate anions commonly known as the scorpionates.[4] Since their introduction in 1966 there has been a steady evolution of these systems. The introduction of steric bulk was quickly achieved, and latterly more limited attention has been given to their electronic properties.[5] We have sought to extend the scope of the scorpionate ligands by developing "soft" tripodal systems such as the hydrotris(methimazolyl)borate anion (Tm^{Me})[6,7] (Scheme 1), replacing the heterocyclic nitrogen donors of hydrotris(pyrazolyl)borate anion (Tp) with thione sulfur donors. Initially, studies using these ligands produced results which were qualitatively in accordance with accepted hard and soft acid/base concepts. For example, it was found to be relatively simple to form soft scorpionate complexes of copper(I),[6,8] but much more difficult to generate the analogous copper(II) species and to this day the simple complexes of copper(II) remain elusive.[9] Furthermore, unlike the nominally hard pyrazole based ligands, our thione

[a] Department of Pure & Applied Chemistry,
University of Strathclyde,
295 Cathedral St., Glasgow G1 1XL, UK
Fax: +44-141-552-0876
E-mail: j.reglinski@strath.ac.uk
m.d.spicer@strath.ac.uk

Supporting information for this article is available on the WWW under http://www.eurjic.org or from the author.

donor ligands readily form a range of stable complexes of the lower main group elements (e.g. Sb, Te and Bi).[10] In the face of these predictable observations, a number of intriguing anomalies began to appear in the behaviour of these soft scorpionates, which did not support the view that their chemistry could be explained purely on the basis of hard and soft acid/base properties.

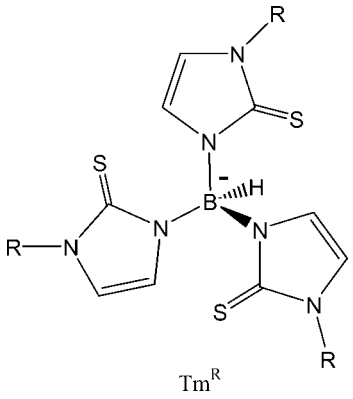

Tm^R

Scheme 1.

It is of interest to compare the three 6e⁻ face capping ligands, Tm, Tp and Cp. While the relative hardness of these ligands would be expected to lie in the order Tp > Cp > Tm^{Me}, most quantitative results obtained placed the ligands in a different order. Thus, in the complexes [$Fe^{II}(L)_2$], there is a transition from low spin (Cp) to spin-crossover (Tp) to high spin (Tm^{Me}) magnetic behaviour, suggesting that the spectrochemical series for these ligands lies in the order Cp > Tp > Tm^{Me}.[11] This is further supported by the cobalt chemistry of these ligands,[12] in which a tetrahedral (weak field) complex [$Co^{II}(Tm^{Me})X$] is obtained with Tm^{Me}, while the stronger field ligands Cp and Tp both form sandwich complexes [$Co^{II}(L)_2$].

Additionally, in our study of the group 6 species ([$Mo(Tm^{Me})(CO)_2(\eta^3\text{-}C_3H_5)$] and [$W(Tm^{Me})(CO)_3I$])[13a] we observed that the carbonyl stretching frequencies of the iodo and η^3-allyl species also lie in the order Cp > Tp > Tm^{Me}, suggesting that Tm is in fact the strongest electron donor of the three tripodal ligands and Cp the weakest. It is notable that Tp, as the moiety which relies on σ interactions, is found in the middle of this short series and not at either of its termini. This has been further supported by other observations. For instance, the reduction potentials of the complexes $[Co^{III}(L)_2]^+$ confirm that the Tm^{Me} complex is the most difficult to reduce, consistent with Tm^{Me} being the strongest electron donor.[12] Furthermore, we found that we were unable to stabilise tin(II) complexes with the Tm^{Me} ligand, obtaining only the tin(IV) adducts. In this situation oxidation occurred even under anaerobic conditions,[10m] thus supporting the idea that the Tm^{Me} ligand is an unusually strong electron donor.

It is clear that our appreciation of the Tm^R ligand system is as yet incomplete. We therefore decided to undertake DFT calculations on an appropriate series of complexes in an effort to extend our understanding of both the ligand and the metal–ligand bonding interaction. The previously studied group 6 (Mo, W) carbonyl complexes seemed ideal for this purpose. However, the unusual geometries of the [$M(Tm^{Me})(CO)_3I$] and [$M(Tm^{Me})(CO)_2(\eta^3\text{-allyl})$] complexes seemed less than ideal and since the more regular octahedral complexes [$M(L)(CO)_2(NO)$] (L = Cp, Tp) are well known and several are structurally characterised, these were chosen. Helpfully, both the CO and NO ligands report (by their C–O and N–O stretching frequencies) on the electronic properties of the complexes. We have prepared the Tm^{Me} analogues, characterised them crystallographically and spectroscopically and have undertaken DFT calculations on each of the complexes. We report here the results of this study.

Results and Discussion

Initially the study set out to produce the complete series of group 6 species, [$M(Tm^{Me})(CO)_2(NO)$] (where M = Cr, Mo or W), using established methods (Scheme 2). The molybdenum and tungsten complexes were isolated and crystallised straightforwardly, albeit in poor yield. The reactions were not optimised, and as discussed below, there is at least one other product from the reaction, which is formed via a competing reaction pathway. In contrast, we were unable to isolate the chromium complex.[14] In retrospect this result is not particularly surprising, as the early reports of the preparation of the group 6 cyclopentadienyl complexes clearly show that a unified synthetic strategy for these compounds does not exist either.[15]

Structural Analysis

The complexes [$M(Tm^{Me})(CO)_2(NO)$] (M = Mo, W) were characterised by X-ray crystallography to reveal the expected structural motifs (Figure 1) in which the Tm^{Me} ligand caps one face of the coordination polyhedron, in keeping with the known Tp and Cp analogues. The metals adopt slightly distorted octahedral coordination geometries (Table 1) and, as previously observed, the ligand bite angles (S–M–S) are on average slightly greater than 90°, while the adjacent angles range from 85.53° to 93.27° for molybdenum and 86.25° to 94.28° for tungsten. Due to the lanthanide contraction and the more efficient overlap of the tungsten d-orbitals with those on sulfur, the M–S distances in

$$M(CO)_6 \xrightarrow{DMF/\Delta} M(CO)_3(DMF)_3 \xrightarrow{NaTm^{Me}} Na[M(Tm^{Me})(CO)_3] \xrightarrow{[NO]BF_4} [M(Tm^{Me})(CO)_2NO]$$

DMF = dimethylformamide, M = Mo, W

Scheme 2.

Table 1. Selected bond lengths [Å] and bond angles [°] for $[Tm^{Me}M(CO)_2NO]$ (where M = Mo or W) obtained by crystallographic and DFT methods.

Bond or angle	$[Mo(Tm^{Me})(CO)_2NO]$ Exp.	Calcd.	$[W(Tm^{Me})(CO)_2NO]$ Exp.	Calcd.	$[Mo(Tp)(CO)_2NO]$ Exp.	Calcd.	$[Mo(Cp)(CO)_2NO]$ Exp.	Calcd.	$[Mo(CO)_2NO]^+$ Calcd.
M–S3	2.5865(7)	2.680	2.5708(7)	2.671					
M–S4	2.5594(6)	2.652	2.5480(7)	2.654					
M–S5	2.5767(7)	2.693	2.5637(8)	2.697					
M–N42	1.901(2)	1.837	1.892(3)	1.851		1.845	1.899	1.848	1.817
M–C40	1.957(3)	2.010	1.920(3)	2.014		2.022	1.957	2.004	
M–C41	1.979(3)	2.007	1.973(3)	2.011		2.022	1.941	2.004	
< M–N–O	176.8(2)	179.2	177.7(2)	179.5		179.1	177.85	175.8	
N–O	1.163(3)	1.193	1.185(3)	1.198		1.190	1.167	1.189	1.166
< M–C–O	176.8(2)	179.5	177.3(3)	179.0		179.5	178.21	177.1	
	177.4(2)	178.5	177.5(3)	179.6		179.5	176.80	177.2	
C–O	1.086(3)	1.167	1.157(3)	1.170		1.165	1.143	1.164	1.150
	1.136(3)	1.166	1.148(4)	1.169		1.165	1.154	1.164	
< S3–M–S5	92.18(2)	91.1	91.66(2)	90.4	N/A				
< S3–M–S4	90.56(2)	90.1	90.24(2)	89.6					
< S4–M–S5	89.29(2)	90.0	88.79(2)	89.7					
< N42–M–C41	93.24(10)	91.8	92.71(12)	91.9		90.8	91.35	93.0	
< N42–M–C40	90.07(10)	90.9	89.43(11)	90.9		90.8	91.79	93.1	
< N42–M–S3	176.03(7)	175.2	176.00(8)	175.9					
< C41–M–S4	86.47(7)	88.4	86.93(8)	88.7					
< C40–M–S5	93.34(7)	90.2	94.27(9)	90.8					

the two complexes are similar, with the Mo–S distances in the molybdenum complex being slightly longer than the equivalent W–S distances. Consistent with the other structures obtained from the metal complexes of this ligand,[6–13] the methimazolyl rings of the Tm^{Me} ligand lie at a mean angle of 33.5° to the imaginary H–B–M axis. This has the effect of reducing the symmetry of the $M(Tm^{Me})$ fragment from C_{3v} to approximately C_3 thus minimising the steric strain in the eight-membered chelate rings.

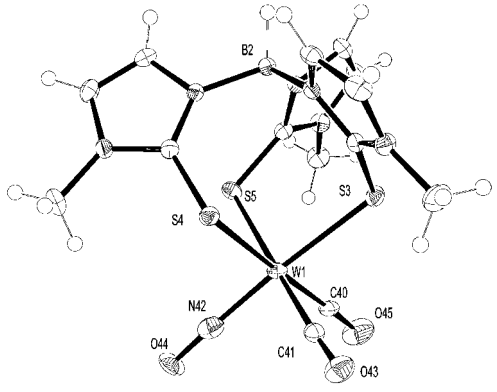

Figure 1. The X-ray crystal structure of $[W(Tm^{Me})(CO)_2(NO)]$. The molybdenum complex (not shown) is isostructural with its heavier congener. The atoms are labelled in a manner consistent with the output from the DFT studies. Thermal ellipsoids are at 50%.

Due to the difficulty in identifying the occupants of the positions associated with the carbonyl carbon atoms and nitrosyl nitrogen in the X-ray structure, the nitrosyl nitrogen was placed in accordance with the results of the DFT calculations (vide infra), i.e. *cis* to the shortest M–S bond. This problem obviates any meaningful comparison with the analogous Tp and Cp systems, which are beset by similar, but irresolvable, problems. Metrical parameters for $[W(Tp)(CO)_2NO]$ and $[W(Cp)(CO)_2NO]$ and the esds for $[Mo(Cp)(CO)_2NO]$ are not available. Values for the $[Mo(CO)_2NO]^+$ ion have been calculated in an attempt to provide information that is independent of the facial ligand.

Although the X-ray crystal structures clearly confirm the identity of the two species, ambiguity remains in that it was not possible to distinguish crystallographically between the C and N atoms of CO and NO. Consequently, the relative positions of the π acid ligands cannot be established beyond doubt. The problem of distinguishing between CO and NO is also evident in the structures of the analogous CpMo[16] and TpMo[17] complexes. Inspection of our structures revealed in each case one of the M–S distances to be shorter than the other two. Intuitively, the unique nitrosyl ligand might be expected to occupy the site *trans* to this bond with the two carbonyl ligands being placed *trans* to the two slightly longer M–S distances, reflecting the relative *trans*-effects of the M–CO and M–NO fragments.

In view of this ambiguity we were interested to apply DFT methods in an attempt to resolve the dilemma. Furthermore, calculations were expected to give insights into a number of aspects of these complexes, including (i) assignment of the CO and NO stretching frequencies in the IR spectrum, (ii) the nature of the M–NO bonding, and (iii) the nature of the metal to tripodal ligand bonds.

DFT Molecular Orbital Calculations

Thus, we have subjected $[M(Tm^{Me})(CO)_2(NO)]$ (M = Cr, Mo, W) and their Tp and Cp analogues to DFT analysis, using the atomic coordinates retrieved from the respective X-ray crystal structures (where available) as a starting point for geometry optimisation (see Supporting Information). While calculations were performed for all nine possible complexes $[M(L)(CO)_2(NO)]$ (M = Cr, Mo, W; L = Tm^{Me}, Tp, Cp) only the data for molybdenum are presented in

Figure 2. Calculated structures of $[Mo(L)(CO)_2NO]$ (from left to right, L absent, i.e. $[Mo(CO)_2NO]^+$, L = Cp, Tp, and Tm^{Me}).

detail here, together with the Tm^{Me} complexes of Cr and W. The remaining data for the chromium and tungsten species are deposited as electronic supporting information, and show remarkably similar structural features and trends (for supporting information see also the footnote on the first page of this paper). Although we have been unable to prepare the complex $[Cr(Tm^{Me})(CO)_2(NO)]$ the calculations suggest there is no inherent instability of the complex provided an appropriate synthetic route can be devised. In addition, calculations on the fragment $[Mo(CO)_2(NO)]^+$, without the face capping ligand, were performed for comparative purposes.

The three calculated structures for the molybdenum complexes $[Mo(L)(CO)_2(NO)]$ (Figure 2) are found to maintain the same gross features as the crystallographic structures presented in Figure 1 and Table 1. It is interesting that for the Tm^{Me} complexes they indicate that the NO ligand should lie *cis*- to the shortest M–S bond (rather than *trans*). We have subsequently refined the X-ray data in light of this observation to give acceptable convergence and structural parameters. However, as expected there are some deviations (up to 4% difference) between the crystallographically determined and calculated bond lengths and angles in all three species. These differences are seen most markedly in the metal-coordination sphere, where calculated M–S distances are ca. 0.1 Å longer than those observed experimentally, and in the π acid ligands, where the M–C, M–N, C–O and N–O distances do not exactly correlate. These differences presumably arise from a combination of factors not least the uncertainty of placing the key atoms in the X-ray structures (NO vs. CO), the approximations in the potentials used for the heavier transition metals, and because the calculations pertain to a gas-phase species in contrast to the solid state structural data. Nevertheless, consistent trends are observed giving confidence in the validity of the results.

One interesting feature of the DFT calculations is the infrared frequencies obtained (Table 2), which clearly identify the single NO and two CO stretches observed in these species. Correction factors are often applied to band frequencies in order to obtain acceptable agreement between experiment and theory. In this case no such correction was deemed necessary, as the agreement between the observed and calculated band frequencies is good. Indeed the discrepancies are not appreciably worse than those observed between the infra-red data obtained in the liquid and solid phase. The major divergence between experiment and theory is in the relative intensities of the bands (Table 2). The calculations suggest that the intensities of the three bands should be similar, but experimentally the νNO is significantly (×2) more intense than the νCO.

The hypothetical $[M(CO)_2(NO)]^+$ fragment was generated to allow us to better inspect the influence of the facially capping ligand. The fragment itself is calculated to have an ν(NO) = 1804 cm^{-1} and ν(CO) = 2006 and 2062 cm^{-1}, which reflects the cationic nature of the species. The effect of adding a tripodal ligand to this fragment is to

Table 3. Mulliken Charge Distribution on the nitric oxide ligand in the series of compounds $[ML(CO)_2NO]$ (where M = Mo or W; L = Tm, Tp and Cp).

	Molybdenum		
	Cp	Tp	Tm
Nitrogen	–0.082	–0.102	–0.108
Oxygen	–0.148	–0.156	–0.166
Nitric oxide (sum)	–0.230	–0.258	–0.274
	Tungsten		
Nitrogen	–0.155	–0.155	–0.159
Oxygen	–0.158	–0.167	–0.180
Nitric oxide (sum)	–0.313	–0.322	–0.339

Table 2. The experimental (CH_2Cl_2) and calculated CO and NO stretching frequencies (calculated intensities in parentheses) for the nitrosyl complexes $[M(L)(CO)_2NO]$ (M = Mo or W; L = Tm, Tp and Cp) and for the hypothetical $[Mo(CO)_2NO]^+$ ion. All calculated frequencies (1600–2200 cm^{-1}) are reported.

		$[M(Tm^{Me})(CO)_2NO]$		$[M(Tp)(CO)_2NO]$		$[M(Cp)(CO)_2NO]$		$[Mo(CO)_2NO]^+$
		Obsd.	Calcd.	Obsd.	Calcd.	Obsd.	Calcd.	Calcd.
Mo	νNO	1636	1682 (877)	1666	1702 (912)	1663	1702 (932)	1804
	νCO	1915	1897 (863)	1933	1914 (970)	1937	1920 (1008)	2006
	νCO	2006	1962 (787)	2025	1978 (678)	2020	1978 (613)	2062
		obsd.	calcd.	obsd.	calcd.	obsd.	calcd.	
W	νNO	1614	1669 (877)	1651	1688 (920)	1665	1693 (932)	
	νCO	1886	1855 (912)	1910	1902 (1028)	1925	1913 (1055)	
	νCO	1986	1954 (795)	2010	1968 (723)	2010	1971 (624)	

lower the calculated stretching frequencies by ca. 100 cm^{-1}. This is consistent with the increased electron density at the metal centre, transmitted through classical back-bonding to the NO and CO π* orbitals. The fine detail reveals the relative effects of the individual tripodal ligands. On average, the complexes with the Cp ligand have slightly higher stretching frequencies than those with Tp, while the Tm^{Me} complexes consistently have the lowest stretching frequencies by some 20–30 cm^{-1}. This implies that Tm^{Me} is the most electron-releasing of the three ligands. The trend in IR stretching frequencies is mirrored by the changes in the calculated structural parameters. The N–O and C–O distances show an increase in the order Cp < Tp < Tm^{Me}, while the M–C and M–N distances decrease from Cp through to Tm^{Me}. The Mulliken charge distributions also support this view (Table 3). In each case the negative charge on the nitrosyl oxygen is found to increase Cp < Tp < Tm for molybdenum and tungsten, respectively, indicative of the expected decrease in overall cationic character of the nitrosyl ligand. Thus the calculations, combined with the experimental vibrational spectra, confirm Tm to be the most electron-donating of the three face-capping ligands.

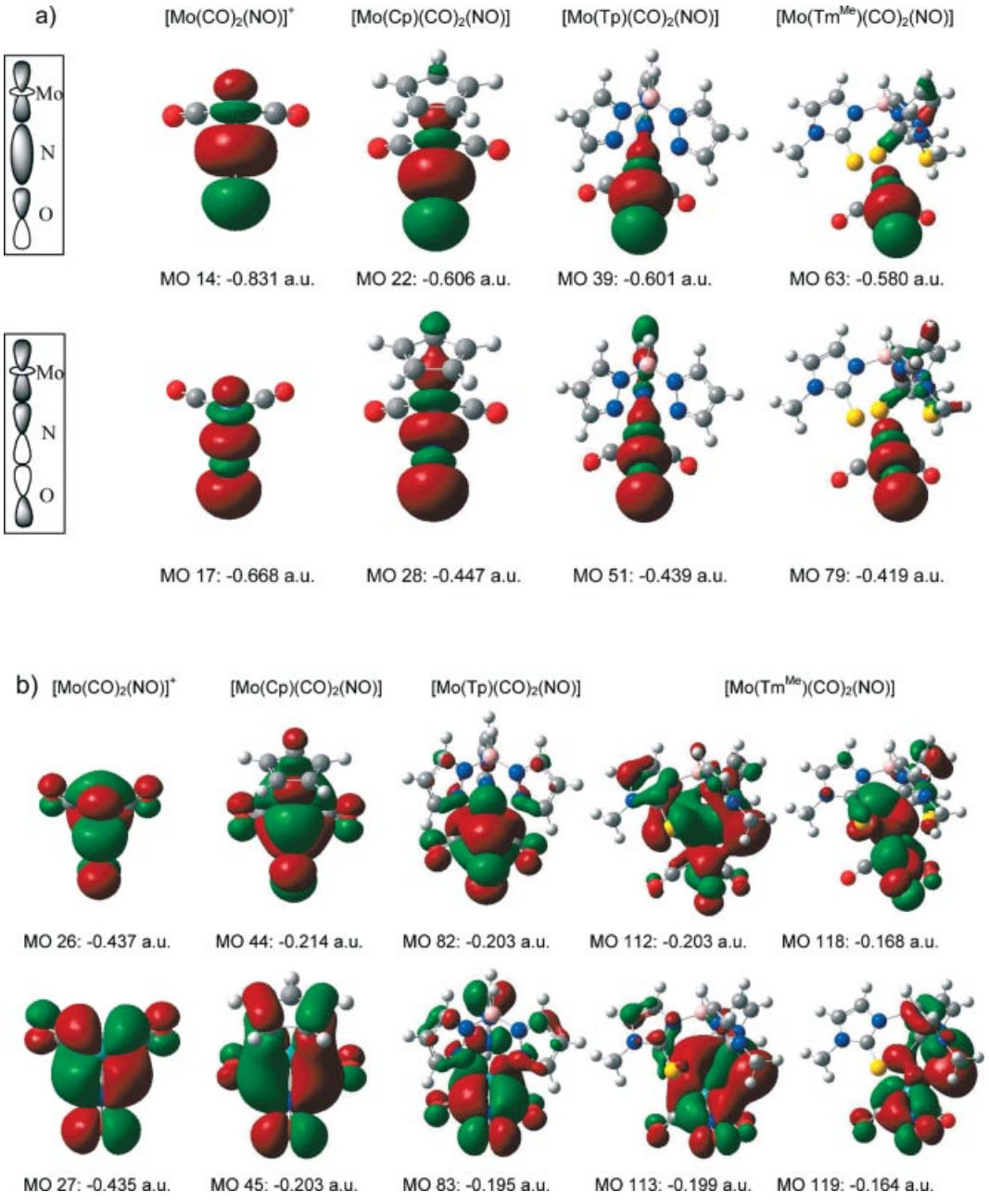

Figure 3. Calculated MOs describing a) the metal to NO σ bonding and b) the metal to NO π back-bonding in $[Mo(CO)_2(NO)]^+$, and $[Mo(L)(CO)_2(NO)]$ (L = Cp, Tp and Tm^{Me}). The symmetry of the Tm^{Me} adducts are lower than the corresponding Tp and Cp species. Consequently the calculations reveal that Tm^{Me} has two π* molecular orbitals of suitable energy for each of those identified for Tp and Cp.

Although the nitrosyl stretching frequencies of $[M(L)(CO)_2(NO)]$ (M = Mo, W; L = Tm^{Me}, Tp, Cp) place them within the range observed for bent nitrosyl ligands (1525–1690 cm^{-1}), it is evident from the DFT calculations and crystallographic studies, that the M–N–O moiety remains linear (<M–N–O 179° calcd.). The observed NO stretching frequency in $[W(Tm^{Me})(CO)_2(NO)]$ at 1614 cm^{-1} is amongst the lowest values yet recorded for a linear NO ligand (1600 cm^{-1}).[18,19] This prompted us to examine the metal-nitrosyl bonding in more detail (Figure 3). In the absence of tripodal ligands, the description of the M–NO bonding derived from the DFT calculations confirms the accepted σ donor, π acceptor model. The NO ligand lies on the *z* axis and the d_{z^2} orbital overlaps with nitrogen s and p orbitals to form the σ bond. The π component of the bonding involves interaction of d_{xz} and d_{yz} orbitals with the orthogonal sets of π* orbitals on NO. Furthermore, there appears to be significant overlap of the CO π* orbitals with the d_{xy} orbital. The calculated ν(NO) is 1804 cm^{-1}, clearly in the region normally associated with linear NO ligands.

On addition of the facially capping ligands to the $[Mo(CO)_2(NO)]^+$ fragment, the bonding picture is largely maintained. However, in the cases of Cp and Tm^{Me} there are significant interactions between the M–NO bonding orbitals and orbitals on the tripodal ligands. Furthermore, the loss of the plane of symmetry in the case of the Tm^{Me} ligand, further complicates the picture. We have selected the major metal–ligand bonding orbitals in the $[M(CO)_2(NO)]^+$ fragment, identified the most closely corresponding orbitals in the $[M(L)(CO)_2(NO)]$ complexes and plotted their energies (Figure 4). On complexation of the face-capping ligand the species becomes electrically neutral and thus there is an increase in the orbital energies relative to the positively charged $[M(CO)_2(NO)]^+$ fragment. It must be argued that the overall effect of complexation of the ligand will be to stabilise this fragment via the bond energies associated with the formation of three extra M–S bonds. However, the rise in orbital energies reflects a destabilisation of the metal/π acid bonding. This is consistent with the weakening of C–O and N–O bonds in the accepted σ-donor π-(acceptor) bonding model. The DFT calculations also allow us an intriguing view of the key molecular orbital interactions in the three metal fragments CpM, TpM and TmM (Figure 3). Consistent with the work of Bergman et al.,[20] Joshi et al.,[21] and Nemykin & Basu,[22] the interactions between Tp and the metal seem to be predominantly directed through nitrogen-based σ donor interactions only and that the influence of the ligand on the ancillary π acid ligands is through these remote interactions. On the other hand, the CpMo fragment indicates significant, direct π overlap between the facially capping ligand and orbitals on

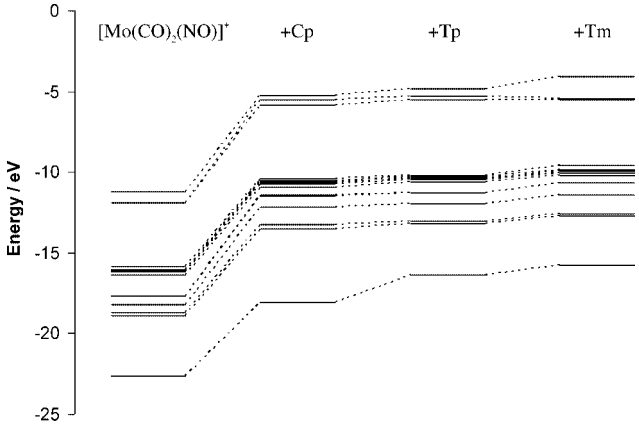

Figure 4. Perturbation of the Mo–π acid ligand bonding on addition of tripodal ligands to the $[Mo(CO)_2(NO)]^+$ fragment.

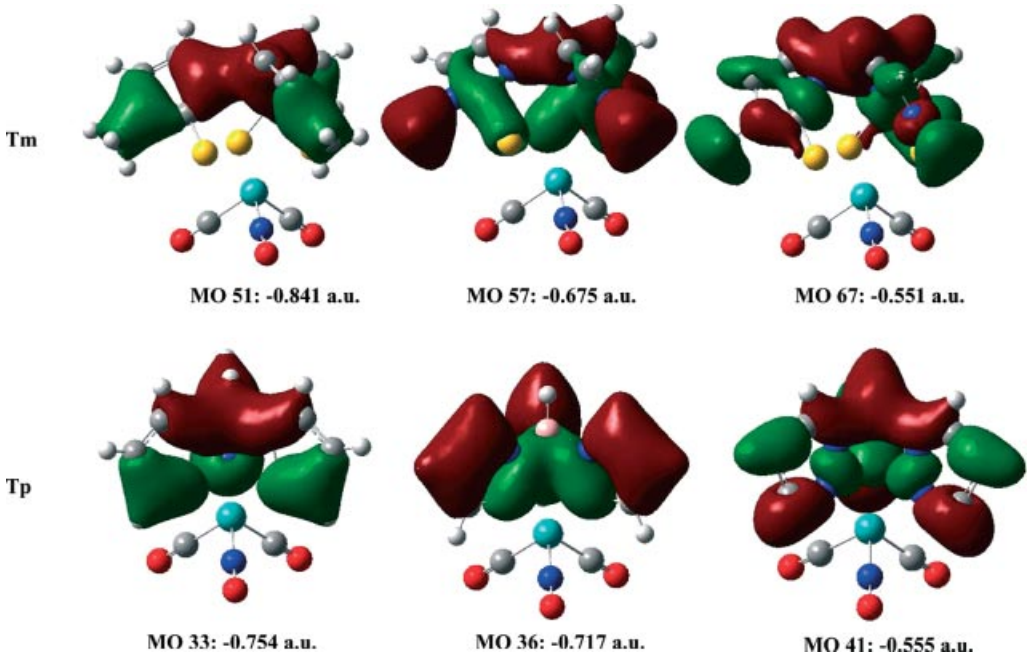

Figure 5. A selection of DFT derived orbitals depicting delocalisation through the Tm^{Me} and Tp Ligands.

the π acid ligands (NO, CO) indicating that strong synergistic bonding operates through the metal centre. The molecular orbitals generated for Tm are more complex than both Cp and Tp, in part because of the lower symmetry and in part because there are significantly more atoms. The sulfur–metal interaction is also considerably more complex than the corresponding nitrogen–metal interaction in Tp complexes. This arises from the presence of predominantly p orbital lone pairs based on sulfur. The π interaction of the sulfur p orbitals with the metal to π acid backbonding orbitals (e.g. MO 113, Figure 3) suggests that the sulfur donor has a direct influence on the nitric oxide ligand. This observation may go some way to explaining why the M–NO fragment remains linear but has a very low stretching frequency.

The DFT calculations also give us an insight into the behaviour of the B–H and the heterocyclic moieties in Tm and Tp. As reported by Joshi et al. for Tp systems,[21] the Tm ligand also shows extensive delocalisation of the heterocyclic rings through boron (Figure 5). In effect each of these ligands has an extended π system which allows electronic communication throughout the ligand. Thus the calculations suggest that the substituents placed on the methimazolyl nitrogen (methyl in Tm^{Me}), and on the bridgehead boron atom, will have a significant influence on the donor properties of the ligand, perhaps greater than has hitherto been recognised.

Thus the DFT calculations confirm that the electron-donor properties ($Tm^{Me} > Tp > Cp$) of these three face-capping ligands are dominated by their bonding mode. The σ donor, π donor bonding of Tm is consistent with the lowest CO and NO stretching frequencies in these complexes, but also with the weak field behaviour observed in other systems.[11,12] Likewise, the simple σ donor Tp to metal interactions and the weak π acceptor properties of Cp are also consistent with the ordering of their properties. It is clear that the term "soft" in relation to the Tm^R ligands is useful. However, this label effectively disguises the view that these ligands can be exceptionally strong electron donors.

An Alternative Reaction Pathway

The overall yields of the reactions conducted in this work were low. This was in part due to the lack of priority in optimising them. However, it was also evident that the nitrosonium cation was not restricted to reacting at the metal centre alone. As a small oxidising agent it is also capable of reacting at the reducing borohydride group, producing a simple borane (Scheme 3), which is trapped by the DMF to produce the novel, neutral DMF adduct of tris(methimazolyl)borane (Figure 6). Although this species was only a minor by-product from the reaction containing molybdenum, it was a significant proportion of the product from the tungsten reaction. The boron-centred molecule maintains many of the structural features of the Tm anion. The three sulfur atoms revert to a position above the BN_3 plane, with the methimazoles adopting a C_3-symmetric propeller conformation around the B–O axis reminiscent of the orientation in the crystal structure of the free parent Tm^{Me} anion.[7] The presence of the large DMF unit does however somewhat reduce the angle that the heterocyclic rings adopt to the main B–O axis. Oxidation of the anion and removal of the small negatively charged hydride leaves the borane with less electron density to distribute around the $B(mt)_3$ moiety, an effect which is evident in the C=S bond lengths, which are much shorter (i.e. have greater double-bond character) than those in the parent Tm^{Me}. If the parent Tm^{Me} anion is considered to be a facially capping six electron donor analogous to Cp and Tp, then this new DMF adduct, being neutral, can be considered as an arene analogue.

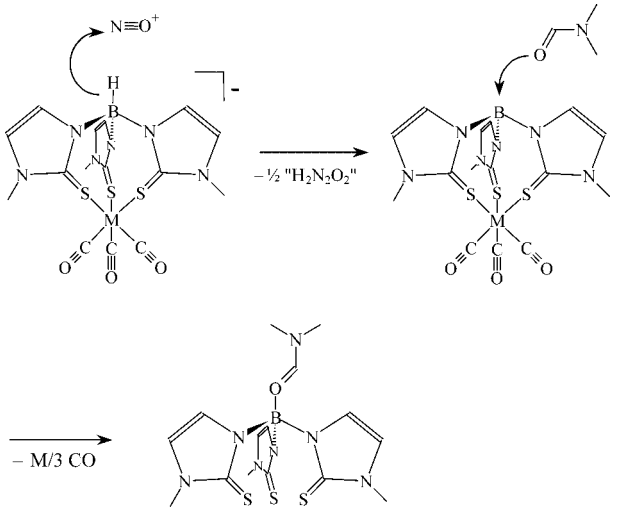

Scheme 3.

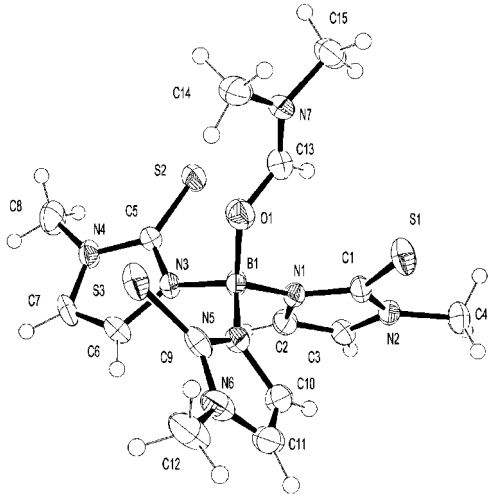

Figure 6. X-ray crystal structure of the dimethylformamide adduct of tris(methimazolyl)borane. Thermal ellipsoids are at 50%.

While the B–H moiety rarely reacts in Tp chemistry, it is not uncommon for it to do so in Tm^R chemistry. Hill has identified two related products which stem from the same reaction profile, namely a cyclic species and an elegant series of metal boratranes.[23] We have observed additional species in these reactions and, because these "degradative"

pathways are of interest in themselves, they will be discussed in greater detail in a subsequent report. In conclusion the data supports the view that Tm^{Me} is a strong π donor and that its character, i.e. its softness, is tempered by the nature of the bonding in the complex. This observation sets it apart from the anionic tripodal phosphanyl borate[24] and thioalkyl borates[5,8a–8c] and as such we can expect to continue seeing greater diversity within this sub grouping of the scorpionate species.

Experimental Section

Unless otherwise stated all experiments were carried out using standard Schlenk techniques and commercially available chemicals. Hexane, THF and diethyl ether were dried and distilled from potassium under dinitrogen. Dichloromethane was dried and distilled from calcium hydride under dinitrogen. Dimethylformamide was dried with molecular sieves (4 Å) prior to distillation at reduced pressure. NMR analysis was carried out with a Bruker AMX 400 operating at 400 MHz for proton and 100 MHz for carbon. Infrared spectra were recorded as potassium bromide discs or in solution (dichloromethane) with a Nicolet Avatar 360 FT-IR spectrometer. Sodium hydrotris(methimazolyl)borate ($NaTm^{Me}$) was prepared using published methods.[6,7]

Preparation of [Dicarbonyl(nitrosyl)hydrotris(methimazolyl)borato]-molybdenum: Hexacarbonylmolybdenum (0.26 g, 1.0 mmol) was dissolved in dimethylformamide (20 mL) under dinitrogen. The reaction mixture was refluxed gently for 20 h whereupon the solution became very dark in colour. The solution was cooled to room temperature and $NaTm^{Me}$ (0.40 g, 1.1 mmol) added. The solution was stirred for 24 h after which time an equimolar amount of nitrosonium tetrafluoroborate (0.12 g, 1.0 mmol) was added. The solution was stirred for a further 2 h during which time gas evolution (CO) was evident. The DMF was removed by vacuum distillation and the product extracted into THF (3 × 40 mL), filtered through celite and stored at –20 °C overnight. The solution separated into a black tar and an orange liquor. The liquors were refiltered and reduced in volume and returned to the freezer at –20 °C. Over a 48-h period a crop of red crystals formed. These were collected by aspirating the liquors from the Schlenk tube thus leaving the desired material in the flask. Crystals suitable for X-ray analysis were removed from the sample prior to drying at reduced pressure overnight. Yield: 0.08 g, 15%. $C_{14}H_{16}BMoN_7O_3S_3$ (533.26): calcd. C 31.53, H 3.02, N 18.39; found C 32.13, H 3.87, N 18.57. ^{1}H NMR (400 MHz, [D$_6$]DMSO): δ = 7.34 (dd, 2 H, –CH=), 7.30 (d, J = 2.1 Hz, 1 H, CH), 7.04 (d, J = 2.1 Hz, 1 H, CH), 7.02 (d, J = 2.1 Hz, 1 H, CH), 6.97 (d, J = 2.1 Hz, 1 H, CH), 3.61 (s, 3 H, CH_3), 3.56 (s, 3 H, CH_3), 3.50 (s, 3 H, CH_3) ppm. IR (KBr disc): $\tilde{\nu}$ = 2468 (weak, BH), 1995 (strong, CO), 1898 (strong, CO), 1630 (strong, NO), 736 (m, C=S), (CH_2Cl_2): $\tilde{\nu}$ = 2006 (strong, CO), 1915 (strong, CO), 1636 (strong, NO) cm^{-1}.

Preparation of Dimethylformamido(trismethimazolyl)borane and [Dicarbonyl(nitrosyl)hydrotris(methimazolyl)borato]tungsten: Hexacarbonyltungsten (0.70 g, 2.0 mmol) was dissolved in dimethylformamide (20 mL) under dinitrogen. The reaction mixture was refluxed gently for 20 h whereupon the solution became very dark green. The solution was cooled to room temperature and $NaTm^{Me}$ (0.75 g, 2.0 mmol) added. The solution was stirred for 48 h after which time an equimolar amount of nitrosonium tetrafluoroborate (0.24 g, 2.0 mmol) was added. The solution was stirred for a further 4 h during which time gas evolution (CO) was evident. The DMF was removed by vacuum distillation and the product extracted into THF (3 × 40 mL), filtered through celite, reduced in volume by 60% and stored at –20 °C overnight whereupon a crop of pale orange crystals formed. These were collected by aspirating the liquors from the Schlenk tube. Crystals for X-ray analysis were removed from the sample prior to drying at reduced pressure overnight. These were found to be an intriguing and significant side product. Yield: 70 mg, 8%. $C_{15}H_{22}BN_7OS_3$ (423.38): calcd. C 42.54, H 5.24, N 23.16; found C 41.22, H 3.90, N 23.46. ^{1}H NMR (400 MHz, $CDCl_3$): δ = 8.70 (s, 1 H, –CHO), 6.68 (d, J = 2.3 Hz, 3 H, CH), 6.46 (br. s, 3 H, CH), 3.59 (s, 9 H, CH_3), 3.32 (s, 3 H,

Table 4. Crystallographic data.

	[Mo(Tm^{Me})(CO)$_2$(NO)]·2THF	[W(Tm^{Me})(CO)$_2$(NO)]·2THF	[B(mt)$_3$(DMF)][a]
Empirical formula	$C_{22}H_{32}B_1MoN_7O_5S_3$	$C_{22}H_{32}B_1N_7O_5S_3W$	$C_{15}H_{22}B_1N_7O_1S_3$
M_w	677.48	765.39	423.40
T [K]	123	123	123
Crystal system	monoclinic	monoclinic	monoclinic
Space group	$P2_1/n$	$P2_1/c$	$P2_1/c$
a [Å]	9.23550(10)	9.2298(2)	7.5076(1)
b [Å]	17.4571(2)	17.4031(3)	12.6102(2)
c [Å]	17.8692(3)	17.8360(4)	25.2145(5)
a [deg]	90	90	90
β [deg]	85.3340(10)	94.6830(10)	92.976(1)
γ [deg]	90	90	90
Z	4	4	4
V [Å^3]	2871.41(7)	2855.38(10)	2384.35(17)
$\mu_{calcd.}$ [mm^{-1}]	0.721	4.311	0.329
F(000)	1392	1520	888
Crystal size [mm]	0.38 × 0.3 × 0.24	0.5 × 0.4 × 0.04	0.4 × 0.4 × 0.3
Radiations	Mo-K_α	Mo-K_α	Mo-K_α
Reflections measured	12788	12008	8960
Unique reflections	6532 (R_{int} = 0.0415)	6468 (R_{int} = 0.0224)	5255 (R_{int} = 0.0267)
Parameters	359	351	249
R[b] [$I > 2\sigma(I)$]	0.0356	0.0252	0.0483
R_w[c] (all reflections)	0.0708	0.0480	0.1388
GOF	1.037	1.074	1.050

[a] mtH = 1-methylimidazole-2-thione (methimazole). [b] $R = \Sigma||F_o| - |F_c||/\Sigma |F_o|$. [c] $R_w = \{\Sigma[w(F_o^2 - F_c^2)^2]/\Sigma[w(F_o^2)^2]\}^{1/2}$.

CH_3), 3.25 (s, 3 H, CH_3) ppm. ^{13}C NMR (100.6 MHz, $CDCl_3$): δ = 165.1 (–CHO), 164.5 (C=S), 121.1 (CH), 118.3 (CH), 40.4 (CH_3), 36.4 (CH_3), 34.8 (CH_3) ppm. IR (KBr disc): $\tilde{\nu}$ = 1679 (strong, C=O), 736 (m, C=S) cm^{-1}.

The aspirated coloured liquors were placed in a clean vessel and the solvent reduced to a minimum and the vessel returned to the freezer. Overnight a crop of red crystals formed which were identified as the desired product. Yield 0.21 g, 17%. $C_{14}H_{16}BN_7O_3S_3W{\cdot}0.25THF$ (621.17): calcd. C 28.18, H 2.84, N 15.34; found C 28.17, H 2.55, N 15.64. ^1H NMR (400 MHz, [D_6]-DMSO): δ = 6.89 (dd, 2 H, –CH=), 6.86 (s, 2 H, CH), 6.85 (d, J = 2.1 Hz, 1 H, CH), 6.82 (d, J = 2.1 Hz, 1 H, CH), 3.75 (s, 3 H, CH_3), 3.72 (s, 3 H, CH_3), 3.69 (s, 3 H, CH_3) ppm. IR (KBr disc): $\tilde{\nu}$ = 2475 (weak, BH), 1975 (strong, CO), 1871 (strong, CO), 1612 (strong, NO), 739, (m, C=S), (CH_2Cl_2): $\tilde{\nu}$ = 1986 (strong, CO), 1886 (strong, CO), 1614 (strong, NO) cm^{-1}.

X-ray Crystallography: Crystals were coated in mineral oil and mounted on glass fibres. Data were collected at 123 K with a Nonius Kappa CCD diffractometer using graphite-monochromated Mo-K_α radiation. The heavy atom positions were determined by Patterson methods and the remaining atoms located in difference electron density maps. Full matrix least-squares refinement was based on F^2, with all non-hydrogen atoms anisotropic. While hydrogen atoms were mostly observed in the difference maps, they were placed in calculated positions riding on the parent atoms. The structure solution and refinement used the program SHELX-97[25] and the graphical interface WinGX.[26] The structure of $B(mt)_3{\cdot}$dmf contained severely disordered solvent molecule (THF), which was compensated for by use of the SQUEEZE algorithm.[27] A summary of the crystallographic parameters is given in Table 4.

Density Functional Theory (DFT) Molecular Orbital Calculations: Calculations were performed using the Gaussian 98 program.[28] The molecular species were subjected to geometry optimisation at the DFT[29] level and the 6-311G** basis set[30] for the atoms C, N, O, S, B and H. For molybdenum and tungsten, the Stuttgart RSC 1997 ECP basis set, augmented by a diffuse s and p functions with a common exponent of 0.005, was used.[31] Preliminary calculations were carried out on [Mo(Cp)$(CO)_2$(NO)] using four different DFT functionals namely BLYP,[32] B3LYP, BP86,[33] and MPW1PW91.[34] The best agreement with respect to the experimental carbonyl and nitrosyl infra-red frequencies was obtained using the BLYP functionals and hence these were used for the rest of the molecules.

Supporting Information (see also the footnote on the first page of this article): X-ray crystallographic data in CIF format and results of DFT calculations (calculated MO orbitals).

CCDC-625101 (for [$B(mt)_3$(DMF)]), -625102 (for [Mo(Tm^{Me})$(CO)_2$NO]) and -625103 (for [W(Tm^{Me})$(CO)_2$NO]) contain the supplementary crystallographic data for this paper. These data can be obtained free of charge from The Cambridge Crystallographic Data Centre via www.ccdc.cam.ac.uk/data_request/cif.

Acknowledgments

We thank the European Union for funding.

[1] a) G. J. Kubas, *J. Chem. Soc., Chem. Commun.* **1980**, 61; b) G. J. Kubas, R. R. Ryan, B. I. Swanson, P. J. Vergamini, H. J. Wasserman, *J. Am. Chem. Soc.* **1984**, *106*, 451; c) G. J. Kubas, *J. Organomet. Chem.* **2001**, *635*, 37.

[2] J. L. Templeton, *Adv. Organomet. Chem.* **1989**, *29*, 1.

[3] C. A. Tolman, *Chem. Rev.* **1977**, *77*, 314.

[4] a) S. Trofimenko, *J. Am. Chem. Soc.* **1966**, *88*, 1842; b) S. Trofimenko, *Scorpionates: The Coordination Chemistry of Polypyrazolylborate Ligands*; Imperial College Press, London, **1999**.

[5] P. H. Ge, B. S. Haggerty, A. L. Rheingold, C. G. Riordan, *J. Am. Chem. Soc.* **1994**, *116*, 8406.

[6] M. Garner, J. Reglinski, I. Cassidy, M. D. Spicer, A. R. Kennedy, *Chem. Commun.* **1996**, 1975.

[7] J. Reglinski, M. Garner, I. D. Cassidy, P. A. Slavin, M. D. Spicer, D. R. Armstrong, *J. Chem. Soc., Dalton Trans.* **1999**, 2119.

[8] a) P. J. Schebler, C. G. Riordan, L. M. Liable-Sands, A. L. Rheingold, *Inorg. Chim. Acta* **1988**, *270*, 543; b) C. Ohrenberg, M. M. Saleem, C. G. Riordan, G. P. A. Yap, A. K. Verma, A. L. Rheingold, *Chem. Commun.* **1996**, 1081; c) C. Ohrenberg, L. M. Liable-Sands, A. L. Rheingold, C. G. Riordan, *Inorg. Chem.* **2001**, *40*, 4276; d) G. G. Lobbia, C. Pettinari, C. Santini, N. Somers, B. W. Skelton, A. W. White, *Inorg. Chim. Acta* **2001**, *319*, 15; e) M. Carei, L. Elviri, M. Lanfranchi, L. Marchio, C. Mora, M. A. Pellinghelli, *Inorg. Chem.* **2003**, *42*, 2109.

[9] C. A. Dodds, M. Garner, J. Reglinski, M. D. Spicer, *Inorg. Chem.* **2006**, *45*, 2733.

[10] a) P. J. Schlebler, C. G. Riordan, I. A. Guzel, A. L. Rheingold, *Inorg. Chem.* **1998**, *37*, 4754; b) J. Reglinski, M. D. Spicer, M. Garner, A. R. Kennedy, *J. Am. Chem. Soc.* **1999**, *121*, 2317; c) B. M. Bridgewater, G. Parkin, *J. Am. Chem. Soc.* **2000**, *122*, 7140; d) P. A. Slavin, J. Reglinski, M. D. Spicer, A. R. Kennedy, *J. Chem. Soc., Dalton Trans.* **2000**, 239; e) C. Kimblin, B. M. Bridgewater, G. Parkin, *J. Chem. Soc., Dalton Trans.* **2000**, 891; f) C. Kimblin, B. M. Bridgewater, T. Hascall, G. Parkin, *J. Chem. Soc., Dalton Trans.* **2000**, 1267; g) P. J. Bailey, M. Lanfranchi, L. Marchio, S. Parsons, *Inorg. Chem.* **2001**, *40*, 5030; h) J. F. Ojo, P. A. Slavin, J. Reglinski, M. Garner, M. D. Spicer, A. R. Kennedy, S. J. Teat, *Inorg. Chim. Acta* **2001**, *313*, 15; i) C. Santini, M. Pellei, G. G. Lobbia, C. Pettinari, A. Drozdov, S. Troyanov, *Inorg. Chim. Acta* **2001**, *325*, 20; j) M. Cammi, M. Lanfranchi, L. Marchio, C. Mora, C. Paiola, M. A. Pellinghelli, *Inorg. Chem.* **2003**, *42*, 1769; k) K. Fujita, A. L. Rheingold, C. G. Riordan, *Dalton Trans.* **2003**, 2004; l) C. A. Dodds, A. R. Kennedy, J. Reglinski, M. D. Spicer, *Inorg. Chem.* **2004**, *43*, 394; m) C. A. Dodds, M. Jagoda, J. Reglinski, M. D. Spicer, *Polyhedron* **2004**, *23*, 445; n) C. A. Dodds, J. Reglinski, M. D. Spicer, *Chem. Eur. J.* **2006**, *12*, 933.

[11] M. Garner, K. Lewinski, A. Pattek-Janczyk, J. Reglinski, B. Sieklucka, M. D. Spicer, M. Szaleniec, *Dalton Trans.* **2003**, 1181.

[12] C. A. Dodds, M. A. Lehmann, J. F. Ojo, J. Reglinski, M. D. Spicer, *Inorg. Chem.* **2004**, *43*, 4297.

[13] a) M. Garner, M.-A. Lehmann, J. Reglinski, M. D. Spicer, *Organometallics* **2001**, *20*, 5233; b) H. P. Kim, S. Kim, R. A. Jacobsen, R. J. Angelici, *Organometallics* **1986**, *5*, 2481; c) R. H. Hill, A. Becalska, N. Chiem, *Organometallics* **1991**, *10*, 2104.

[14] The species isolated from this reaction were organic in nature. These will be discussed elsewhere in a separate report.

[15] a) E. O. Fischer, O. Beckert, W. Hafner, H. O. Stahl, *Z. Naturforsch., Teil B* **1955**, *10*, 598; b) S. Trofimenko, *Inorg. Chem.* **1969**, *8*, 2675.

[16] S.-Y. Yang, W.-H. Sun, Y.-Q. Yin, K.-B. Yu, Z.-Y. Zhou, *Sci. China, Ser. B* **1991**, *34*, 1304.

[17] E. M. Holt, S. L. Holt, F. Cavalito, K. J. Watson, *Acta Chem. Scand. A* **1976**, *30*, 225.

[18] C. A. Reed, W. R. Roper, *J. Chem. Soc. A* **1970**, 3054.

[19] V. G. Albano, P. Bellon, M. Sansoni, *J. Chem. Soc. A* **1971**, 2420.

[20] R. G. Bergman, T. R. Cundari, A. M. Gillespie, T. B. Gunnoe, W. D. Harman, T. R. Klinckmam, M. D. Temple, D. P. White, *Organometallics* **2003**, *22*, 2331.

[21] H. K. Joshi, M. E. Arvin, J. C. Durivage, N. E. Gruhn, M. D. Carducci, B. L. Westcott, D. L. Lichtenberger, J. H. Enemark, *Polyhedron* **2004**, *23*, 429.
[22] V. N. Nemykin, P. Basu, *Inorg. Chem.* **2005**, *44*, 7494.
[23] a) A. F. Hill, G. R. Owen, A. J. P. White, D. J. Williams, *Angew. Chem. Int. Ed.* **1999**, *38*, 2759; b) I. R. Crossley, A. F. Hill, E. R. Humphrey, M. K. Smith, N. Tshabang, A. C. Willis, *Chem. Commun.* **2004**, 1878; c) I. R. Crossley, M. R. S. Foreman, A. F. Hill, A. J. P. White, D. J. Williams, *Chem. Commun.* **2005**, 221.
[24] a) A. A. Barney, A. F. Heyduk, D. G. Nocera, *Chem. Commun.* **1999**, 2379; b) J. C. Peters, J. D. Feldman, T. D. Tilley, *J. Am. Chem. Soc.* **1999**, *121*, 9871; c) T. A. Betley, J. C. Peters, *Inorg. Chem.* **2003**, *42*, 5074.
[25] G. M. Sheldrick, SHELX97 - Programs for Crystal Structure Analysis (Release 97–2). University of Göttingen, institute of inorganic chemistry, Tammanstrasse 4, 37077 Göttingen, Germany, **1998**.
[26] L. J. Farrugia, *J. Appl. Crystallogr.* **1999**, *32*, 837.
[27] P. van der Sluis, A. L. Spek, *Acta Crystallogr., Sect. A* **1990**, *46*, 194.
[28] Gaussian 98, Revision A.9, M. J. Frisch, G. W. Trucks, H. B. Schlegel, G. E. Scuseria, M. A. Robb, J. R. Cheeseman, V. G. Zakrzewski, J. A. Montgomery Jr, R. E. Stratmann, J. C. Burant, S. Dapprich, J. M. Millam, A. D. Daniels, K. Kudin, M. C. Strain, O. Farkas, J. Tomasi, V. Barone, M. Cossi, R. Cammi, B. Mennucci, C. Pomelli, C. Adamo, S. Clifford, J. Ochterski, G. A. Petersson, P. Y. Ayala, Q. Cui, K. Morokuma, D. K. Malick, A. D. Rabuck, K. Raghavachari, J. B. Foresman, J. Cioslowski, J. V. Ortiz, A. G. Baboul, B. B. Stefanov, G. Liu, A. Liashenko, P. Piskorz, I. Komaromi, R. Gomperts, R. L. Martin, D. J. Fox, T. Keith, M. A. Al-Laham, C. Y. Peng, A. Nanayakkara, M. Challacombe, P. M. W. Gill, B. Johnson, W. M. Chen, W. Wong, J. L. Andres, C. Gonzalez, M. Head-Gordon, E. S. Replogle, J. A. Pople, Gaussian, Inc., Pittsburgh PA, **1998**.
[29] W. Kohn, A. D. Becke, R. G. Parr, *J. Phys. Chem.* **1996**, *100*, 12974.
[30] a) A. D. McLean, G. S. Chandler, *J. Chem. Phys.* **1980**, *72*, 5639; b) R. Krishnan, J. S. Binkley, R. Seeger, J. A. Pople, *J. Chem. Phys.* **1980**, *72*, 650.
[31] a) M. Dolg, H. Stoll, H. Preuss, R. M. Pitzer, *J. Phys. Chem.* **1993**, *97*, 5852; b) Basis sets were obtained from the Extensible Computational Chemistry Environment Basis Set Database, Version 02/25/04, as developed and distributed by the Molecular Science Computing Facility, Environmental and Molecular Sciences Laboratory which is part of the Pacific Northwest Laboratory, P. O. Box 999, Richland, Washington 99352, USA, and funded by the U. S. Department of Energy. The Pacific Northwest Laboratory is a multi-program laboratory operated by Battelle Memorial Institute for the U. S. Department of Energy under contract DE-AC06-76RLO 1830. Contact David Feller or Karen Schuchardt for further information. http://www.emsl.pnl.gov/forms/basisform.html.
[32] a) A. D. Becke, *Phys. Rev. A* **1988**, *38*, 3098; b) C. T. Lee, W. T. Yang, R. G. Parr, *Phys. Rev. B* **1998**, *37*, 785.
[33] J. P. Perdew, *Phys. Rev. B* **1986**, *33*, 8822.
[34] a) C. Adamo, V. Barone, *J. Chem. Phys.* **1998**, *108*, 664; b) J. P. Perdew, J. A. Chevary, S. H. Vosko, K. A. Jackson, M. R. Pederson, D. J. Singh, C. Fiolhais, *Phys. Rev. B* **1992**, 46.

Received: November 8, 2006
Published Online: February 22, 2007

